

Rapid Room-Temperature Synthesis and Characterization of Nanocrystals of a Prototypical Zeolitic Imidazolate Framework

Janosch Cravillon,[†] Simon Münzer,[†]
Sven-Jare Lohmeier,[†] Armin Feldhoff,[‡] Klaus Huber,[§]
and Michael Wiebcke*,[†]

Institut für Anorganische Chemie, Leibniz Universität Hannover, Callinstraße 9, D-30167 Hannover, Germany, Institut für Physikalische Chemie und Elektrochemie, Leibniz Universität Hannover, Callinstraße 3A, D-30167 Hannover, Germany, and Department Chemie, Universität Paderborn, Warburger Strasse 100, D-33098 Paderborn, Germany

Received January 19, 2009

Revised Manuscript Received March 16, 2009

We report here a rapid room-temperature colloidal chemistry route to produce nanocrystals with a narrow size distribution of a prototypical zeolitic imidazolate framework (ZIF) material, ZIF-8.^{1,2} ZIFs^{1–7} are a new subclass of porous metal-organic frameworks (MOFs)⁸ in which divalent metal cations are linked by imidazolate anions into tetrahedral frameworks that frequently possess a zeolite topology. Most interestingly, some guest-free ZIFs, e.g., ZIF-8, are reported to exhibit, besides a large intracrystallite surface area, exceptional chemical and thermal stability,¹ a combination of properties rarely to be found among other porous MOF materials. To further tune the properties of ZIFs for specific applications in gas storage, separation, or sensing as well as to make ZIFs available as novel building blocks for advanced nanotechnology devices, it is mandatory to develop synthetic routes for the production of monodisperse nanocrystals.⁹

The chemistry of nanoscale carboxylate-based MOF materials has started to be developed only recently. Direct

mixing,¹⁰ microwave,¹¹ ultrasound,¹² and microemulsion¹³ methods have been used for synthesis and some degree of size and shape control could be achieved. The formation of stable colloidal dispersions of MOF-5 nanocrystals in the presence of a stabilizing monocarboxylate ligand has been monitored in situ by time-resolved static light scattering.¹⁴ Also, nanocrystals of MOFs have been grown on functionalized self-assembled organic monolayers.¹⁵ However, this is the first report on the synthesis and characterization of a nanoscale ZIF material.

It is also remarkable, in comparison with previous syntheses of nanoscale carboxylate-based MOFs,^{10–15} that our simple method does not need any auxiliary stabilizing agents or activation (conventional heating, microwave or ultrasound irradiation) and yields well-shaped ZIF-8 nanocrystals in the form of powders or stable colloidal dispersions. The method relies on pouring at room temperature a methanol solution of $Zn(NO_3)_2 \cdot 6H_2O$ into a methanol solution of the imidazole derivative, 2-methylimidazole (Hmim). It is important to add Hmim in excess to the zinc source, contrary to reported protocols^{1,2} that were designed to produce large microcrystals and used the zinc salt and Hmim in a molar ratio $\leq 1:2$. We obtained good results when employing $Zn(NO_3)_2 \cdot 6H_2O$, Hmim, and methanol in a molar ratio of approximately 1:8:700 (details are provided in the Supporting Information).

Comparison of an X-ray diffraction (XRD) pattern taken from a powder sample with a pattern simulated from known structural data¹ (see Figure S1 in the Supporting Information) demonstrates that the product is single-phase ZIF-8 material. An average particle diameter of 46 nm is estimated from the broadening of the XRD peaks. Secondary electron micrographs (Figure 1a) reveal that the product consists of isometrical nanoparticles with sharp edges and a narrow size distribution. A statistical evaluation of 250 particles results in an average diameter of 40(3) nm. Considering that MOFs are easily damaged in the high-energy electron beam of a transmission electron microscope (TEM),¹⁶ a minimum dose exposure technique was applied for acquisition of high-

* Corresponding author. E-mail: Michael.Wiebcke@acb.uni-hannover.de.

[†] Institut für Anorganische Chemie, Leibniz Universität Hannover.

[‡] Institut für Physikalische Chemie und Elektrochemie, Leibniz Universität Hannover.

[§] Universität Paderborn.

- (1) Park, K. S.; Ni, Z.; Côté, A. P.; Choi, J. Y.; Huang, R.; Uribe-Romo, F. J.; Chae, H. K.; O'Keeffe, M.; Yaghi, O. M. *Proc. Natl. Acad. Sci., U.S.A.* **2006**, *103*, 10186.
- (2) Huang, X.-C.; Lin, Y.-Y.; Zhang, J.-P.; Chen, X.-M. *Angew. Chem., Int. Ed.* **2006**, *45*, 1557.
- (3) (a) Hayashi, H.; Côté, A. P.; Furukawa, H.; O'Keeffe, M.; Yaghi, O. M. *Nat. Mater.* **2007**, *6*, 501. (b) Banerjee, R.; Phan, A.; Wang, B.; Knobler, C.; Furukawa, H.; O'Keeffe, M.; Yaghi, O. M. *Science* **2008**, *319*, 939. (c) Wang, B.; Côté, A. P.; Furukawa, H.; O'Keeffe, M.; Yaghi, O. M. *Nature (London)* **2008**, *453*, 207. (d) Morris, W.; Doonan, C. J.; Furukawa, H.; Banerjee, R.; Yaghi, O. M. *J. Am. Chem. Soc.* **2008**, *130*, 12626.
- (4) Wu, H.; Zhou, W.; Yildrim, T. *J. Am. Chem. Soc.* **2007**, *129*, 5314.
- (5) Tian, Y.-Q.; Zhao, Y.-M.; Chen, Z.-X.; Zhang, G.-N.; Weng, L.-H.; Zhao, D.-Y. *Chem.—Eur. J.* **2007**, *13*, 4146.
- (6) (a) Wu, T.; Bu, X.; Liu, R.; Lin, Z.; Zhang, J.; Feng, P. *Chem.—Eur. J.* **2008**, *14*, 7771. (b) Wu, T.; Bu, X.; Zhang, J.; Feng, P. *Chem. Mater.* **2008**, *20*, 7377.
- (7) Baburin, I. A.; Leoni, S.; Seifert, G. *J. Phys. Chem. Soc.* **2008**, *112*, 9437.
- (8) Yaghi, O. M.; O'Keeffe, M.; Ockwig, N. W.; Chae, H. K.; Eddaoudi, M.; Kim, J. *Nature (London)* **2003**, *423*, 705.
- (9) Tosheva, L.; Valtchev, V. P. *Chem. Mater.* **2005**, *17*, 2494.
- (10) Huang, L.; Wang, H.; Chen, J.; Wang, Z.; Sun, J.; Zhao, D.; Yan, Y. *Microporous Mesoporous Mater.* **2003**, *58*, 105.
- (11) (a) Ni, Z.; Masel, R. I. *J. Am. Chem. Soc.* **2006**, *128*, 12394. (b) Jhung, S. H.; Lee, J.-H.; Yoon, J. W.; Serre, C.; Férey, G.; Chang, J. S. *Adv. Mater.* **2007**, *19*, 121.
- (12) Qiu, L.-G.; Li, Z.-Q.; Wu, Y.; Wang, W.; Xu, T.; Jiang, X. *Chem. Commun.* **2008**, 3642.
- (13) Rieter, W. J.; Taylor, K. M. L.; An, H.; Lin, W.; Lin, W. *J. Am. Chem. Soc.* **2006**, *128*, 9024. (b) Rieter, W. J.; Taylor, K. M. L.; Lin, W. *J. Am. Chem. Soc.* **2007**, *129*, 9852. (c) Daiguebonne, C.; Kerbellec, N.; Guillou, O.; Bünzli, J.-C.; Gumi, F.; Catala, L.; Mallah, T.; Audebrand, N.; Gérald, Y.; Bernot, K.; Clavez, G. *Inorg. Chem.* **2008**, *47*, 3700.
- (14) Hermes, S.; Witte, T.; Hikov, T.; Zacher, D.; Bahnmüller, S.; Langstein, G.; Huber, K.; Fischer, R. A. *J. Am. Chem. Soc.* **2007**, *129*, 5324.
- (15) (a) Hermes, S.; Schröder, F.; Chelmowski, R.; Wöll, C.; Fischer, R. A. *J. Am. Chem. Soc.* **2005**, *127*, 13744. (b) Biemmi, E.; Scherf, C.; Bein, T. *J. Am. Chem. Soc.* **2007**, *129*, 8054.
- (16) (a) Lebedev, O. I.; Millange, F.; Serre, C.; Van Tendeloo, G.; Férey, G. *Chem. Mater.* **2005**, *17*, 6525. (b) Turner, S.; Lebedev, O. I.; Schröder, F.; Esken, D.; Fischer, R. A.; Van Tendeloo, G. *Chem. Mater.* **2008**, *20*, 5622.

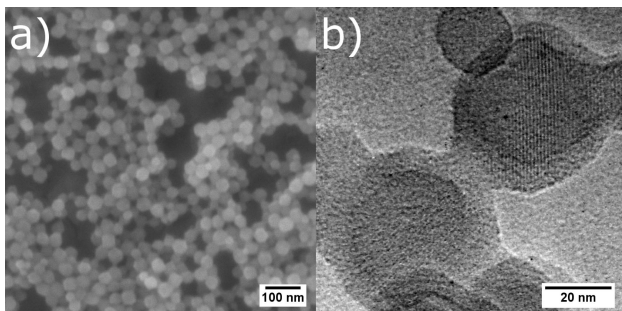


Figure 1. ZIF-8 nanocrystals prepared in methanol. (a) SEM micrograph, (b) HRTEM micrograph showing nanocrystals that exhibit lattice fringes of ca. 1.2 nm that correspond to the (110) family of planes.

resolution TEM (HRTEM) micrographs (Figure 1b). The nanocrystals were oriented on the TEM grid so that they exhibit predominantly (110) lattice fringes. Thus, the nanocrystals are approximately imaged almost along the [001] direction, and their approximate hexagonal envelope then indicates that the particles actually have the shape of a rhombic dodecahedron, that is a {110} crystal morphology (see Figure S3 in the Supporting Information).

Early stages of nanocrystal formation could be successfully monitored *in situ* by time-resolved static light scattering (TR-SLS). Because of the high refractive index of the nanoparticles and their rapid growth, the solutions had to be diluted for these experiments. As shown in Figure 2 for the 1:5:1000 Zn:Hmim:MeOH molar ratio, ca. 130 s after mixing the component solutions, particles with a radius of gyration R_g of ca. 20 nm had been formed. During the 170 s following, the weight averaged particle mass M_w increased further, whereas the corresponding size of the particles remained essentially constant in this growth period. This apparent contradiction can be explained by means of the different averages of the R_g and M_w values, respectively.

The radius of gyration R_g is a square root of the z-averaged squared radius of gyration $\langle S^2 \rangle_z$

$$R_g^2 = \langle S^2 \rangle_z = \frac{\sum_i n_i M_i^2 \langle S_i \rangle}{\sum_i n_i M_i^2}$$

and the molar mass value M_w is a weight averaged value.

$$M_w = \frac{\sum_i n_i M_i^2}{\sum_i n_i M_i}$$

In both averages, i denotes the number of elementary units forming a nanoparticle and n_i and M_i are the number and the molar mass of this nanoparticle, respectively. The scattering signals average over all species of nanoparticles with variable i including elementary units or monomers, which are not yet incorporated into particles. A situation with the size values staying constant but with mass values increasing is observed if single particles grow very fast compared to the duration of our time-resolved experiment. In such a case, the mass fraction of nanoparticles does not increase because of a growth of particles with time but because of an increase in the number of particles due to a

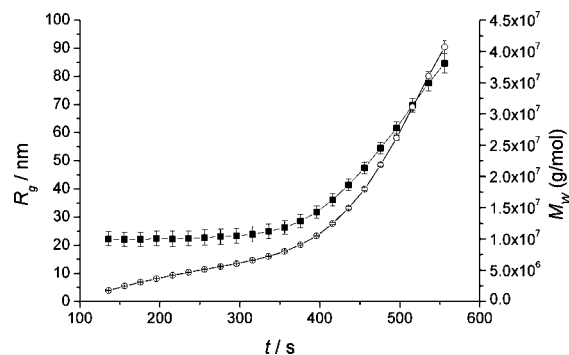


Figure 2. Growth of ZIF-8 nanocrystals in methanol (1:5:1000 Zn:Hmim:MeOH). Radius of gyration R_g vs time (squares) and weight-averaged particle mass M_w vs time (spheres).

continuous nucleation. Such a process still affects the weight average of the mass, whereas the higher z-average of the squared size has already reached its final value. The results thus indicate the existence of an intermediate (primary) nanocrystal with $R_g \approx 20$ nm, which by assuming a spherical particle corresponds to a diameter of ~ 50 nm ($R_{\text{sphere}} = (5/3)^{1/2} R_g$). This nicely agrees with the XRD and TEM results.

Beyond 300 s, both the particle size and mass further increased, indicating an acceleration of the growth process, which likely is due to an agglomeration of primary nanocrystals. A correlation between the radius of gyration and the corresponding mass in this regime of agglomeration led to a power law behavior for $R_g \sim M_w^a$ with an exponent of $0.65 < a < 0.75$. This exponent is well above the value of a compact sphere or cube ($a = 1/3$) and indicates a fractal dimension $1/a$ that corresponds to a loose aggregate of constituent nanocrystal particles. During syntheses, it was observed that sedimentation from the milky synthesis mixtures occurred only very slowly.

Stable, slightly turbid colloidal dispersions were obtained by redispersing the nanocrystals in methanol and studied by dynamic light scattering (DLS) as well as small-angle X-ray scattering (SAXS). A hydrodynamic diameter of 49 nm and a polydispersity index (PDI) of 0.09 were obtained by DLS (see Figure S5 in the Supporting Information), whereas the SAXS data show that isometrical nanoparticles with an average $R_g = 20.4(7)$ nm are present (see Figure S6 in the Supporting Information).

Thermogravimetry (TG) performed on a nanoscale ZIF-8 powder sample (see Figure S7 in the Supporting Information) and temperature-dependent powder XRD (see Figure S8 in the Supporting Information) reveal that in air the nanocrystals are stable up to ca. 200 °C before decomposition of the framework structure takes place. Thus, nanoscale ZIF-8 exhibits considerable thermal stability although it is, as one would expect, of lower thermal stability than microscale ZIF-8 (up to ca. 400 °C in air,² and up to ca. 550 °C in N₂¹). Permanent microporosity of the nanoscale ZIF-8 powder is demonstrated by gas sorption analyses (see Figure S9 in the Supporting Information). From the N₂ sorption isotherms (Figure 3), an apparent specific surface area of 962 m²/g (BET method) and a micropore volume of 0.36 cm³/g are estimated for the evacuated nanocrystals. These values are

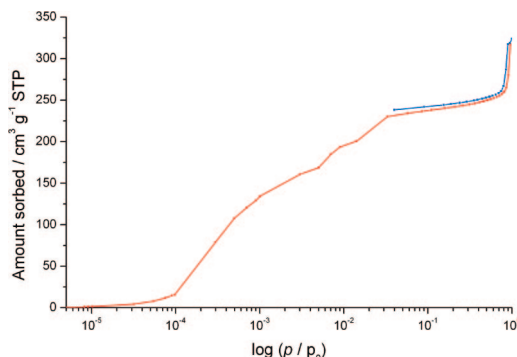


Figure 3. ZIF-8 nanocrystals prepared in methanol. Nitrogen sorption isotherms shown as linear–log plot in order to emphasize the low-pressure range. Adsorption and desorption branch are represented as red and blue curves, respectively.

lower than the highest values reported recently for microscale ZIF-8 (BET surface area: 1630 m²/g, micropore volume: 0.64 cm³/g).¹

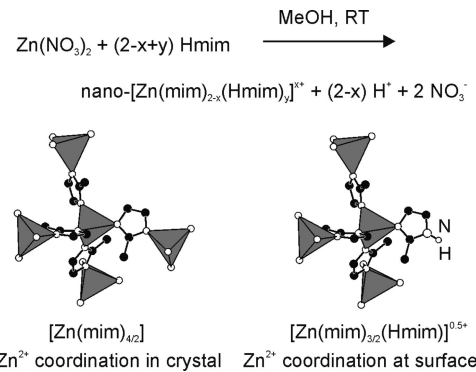
This possibly indicates that the as-synthesized nanoscale ZIF-8 still contains some residual species (e.g., unreacted Hmim) that could not be desorbed from the cavities of the nanocrystals during the activation step before the sorption measurements.

Taking together, our rapid and cheap (regarding chemicals and energy) synthetic protocol yields pure-phase nanoscale ZIF-8 material with a narrow size distribution, good thermal stability, and large accessible internal surface area. Such preformed nanocrystals should be excellent candidates for the preparation of supported ZIF films and membranes, as known for zeolites.¹⁷ Also, nanoscale microporous adsorbents and catalysts are favorable over microscale ones with regard to the mass and energy transport properties.⁹ This could be particularly beneficial for ZIF materials, which frequently possess large cavities that are connected by small apertures (as in the case of ZIF-8, ZIF-95, and ZIF-100), resulting in slow adsorption kinetics when microscale powders are used.^{3c}

We explain the formation of ZIF-8 nanocrystals with the excess of Hmim employed in the syntheses (Scheme 1).

Hmim can act both as a linker unit in its deprotonated form and as a stabilizing unit in its neutral form. If one takes

Scheme 1. Synthesis of ZIF-8 Nanocrystals Capped with Neutral 2-Methylimidazole (Hmim)



the pK_{a1} (7.1) and pK_{a2} (14.2) values for imidazole¹⁸ as a rough estimate for the acid–base properties of Hmim in methanol, one would expect that an equilibrium of the cationic (protonated) and neutral forms exists in solution and deprotonation of Hmim is only driven by the crystallization of ZIF-8 (gain of lattice energy). Enough neutral Hmim should then be available in solution for terminating growth and stabilizing positively charged nanocrystals. This is supported by the value (+55 mV) measured for the ζ potential of stable dispersions of ZIF-8 nanocrystals in methanol. This line of arguments suggests that our method of excess protic linker might be a general one and transferable to other ZIFs, and even carboxylate-based MOFs at low pH conditions.

Acknowledgment. Funding by the Deutsche Forschungsgemeinschaft (DFG) within the frame of the Priority Program 1362 (Porous Metal Organic Frameworks) is gratefully acknowledged.

Supporting Information Available: Experimental details as well as XRD, STEM, TR-SLS, DLS, SAXS, TG/DTA, temperature-dependent XRD, N₂, and Ar gas sorption data (PDF). This material is available free of charge via the Internet at <http://pubs.acs.org>.

CM900166H

(17) (a) Snyder, M. A.; Tsapatsis, M. *Angew. Chem., Int. Ed.* **2007**, *46*, 7560. (b) Caro, J.; Noack, M. *Microporous Mesoporous Mater.* **2008**, *115*, 215.

(18) Sundberg, R. J.; Martin, R. B. *Chem. Rev.* **1974**, *47*, 471.